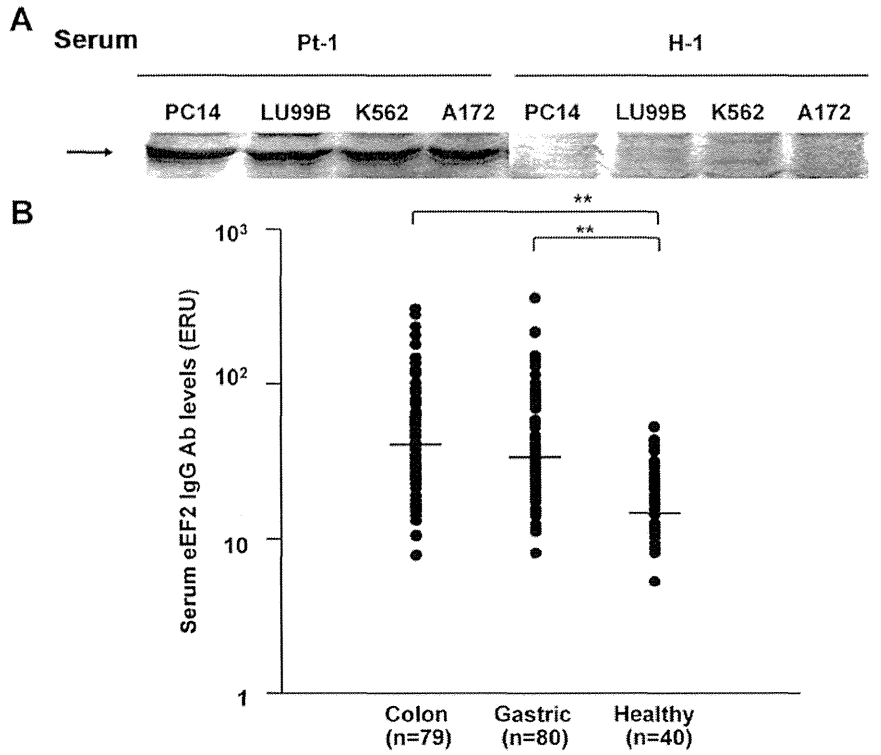

Figure 1. Elevation of serum eEF2 IgG autoantibody levels in cancer patients. (A) Cytoplasmic proteins from PC14, LU99B, K562 and A172 cells were subjected to immunoblot analysis using sera as the first antibodies. Representative results with sera from an HNSCC patient (Pt-1) and a healthy control individual (H-1) are shown. Arrows indicate the protein that is recognized by IgG autoantibody in the sera from the HNSCC patient. (B) Elevation of serum eEF2 IgG autoantibody levels in cancer patients. Assays were performed in duplicate. Colon, colorectal cancer; gastric, gastric cancer; and healthy, healthy individuals. Standard bar represents median value. **p<0.01. eEF2 Ab levels that produces the absorbance at 450 nm equal to that produced by 1 μg/ml of anti-eEF2 H-118 Ab in the ELISA system were defined as 1.0 eEF2-reacting-unit (ERU).

Results

Production of IgG autoantibody against eukaryotic elongation factor 2 (eEF2) in cancer patients. To identify novel tumor-associated antigens (TAAs) with high molecular weight (more than 100 kDa), which were difficult to isolate by standard two dimensional electrophoresis methods because they could not be absorbed into a strip gel, proteins from tumor lysates were first separated by SDS-PAGE, transferred to PVDF membrane, and then probed with sera from tumor-bearing patients. As shown in Fig. 1A, an approximately 100 kDa protein was recognized by sera from 4 of 10 HNSCC and 2 of 3 colon cancer patients in cytoplasmic proteins from two lung cell lines (PC14 and LU99B), one leukemic cell line (K562) and one glioblastoma cell line (A172), whereas it was not recognized by the sera from 5 healthy individuals. To identify this protein, cytoplasmic proteins of K562 cells were fractionated by density gradient isoelectric focusing, separated by SDS-PAGE, and subjected to immunoblot analysis using sera from an HNSCC patient as the first antibody. Since immunoblot analysis detected this protein in fractions of pH 6.62 and pH 6.75, the silver-stained band corresponding to this protein was excised from the SDS-PAGE gel and the protein was analyzed by MALDI-TOF Mass Spectrometry. The search for NCBInr database by MS-Fit software identified the protein as human eukaryotic elongation factor 2 (eEF2) that had M.W. of 95.3-kDa and calculated pI of 6.4.

Elevation of serum eEF2 IgG antibody levels in cancer patients. Serum eEF2 IgG Ab levels were examined by ELISA in 79 colorectal and 80 gastric cancer patients and 40 healthy individuals and detected in all the samples examined (Fig. 1B). eEF2 IgG Ab levels ranged from 7.8 to 301.7 (median 41.1), from 8.1 to 353.9 (median 33.6) and from 5.2 to 53.0 (median 20.6) ERU in colorectal and gastric cancer patients and healthy individuals, respectively. eEF2 IgG Ab levels were significantly ($p<0.01$) higher in both colorectal and gastric cancer patients than healthy individuals.

Overexpression of eEF2 in various types of human cancers. eEF2 protein was immunohistochemically examined in 51 lung cancers, 15 esophageal squamous cell carcinomas, 21 HNSCCs, 28 pancreatic cancers, 8 breast cancers, 16 glioblastoma multiformes, 4 prostate cancers and 50 NHLs. Immunohistochemical analysis with two different anti-EF2 antibodies recognizing different regions of eEF2 protein showed similar results. Overexpression of eEF2 protein was detected in 71.0% (22 of 31) of lung adenocarcinoma, 95.0% (19 of 20) of small-cell lung cancer, 73.3% (11 of 15) of esophageal cancer, 60.7% (17 of 28) of pancreatic cancer, 50.0% (4 of 8) of breast cancer, 75.0% (3 of 4) of prostate cancer, 52.4% (11 of 21) of HNSCC, 75.0% (12 of 16) of glioblastoma multiformes, and 94.0% (47 of 50) of NHL. Results are summarized in Table I. Representative results are shown in Fig. 2.

Table I. Overexpression of eEF2 in human cancers.

Cancer	Overexpression of eEF2 (%)
Lung cancer	80.4 (41/51)
Lung adenocarcinoma	71.0 (22/31)
Small cell lung cancer	95.0 (19/20)
Esophageal squamous cell carcinoma	73.3 (11/15)
Head and neck squamous cell carcinoma	52.4 (11/21)
Pancreatic cancer	60.7 (17/28)
Breast cancer	50.0 (4/8)
Glioblastoma	75.0 (12/16)
Prostate cancer	75.0 (3/4)
Non-Hodgkin's lymphoma	94.0 (47/50)
Diffuse large B cell lymphoma	92.5 (37/40)
Follicular lymphoma	100 (10/10)

Expression of eEF2 protein in human cancers was examined by immunohistochemistry. Immunostaining was evaluated as positive when cancer cells were stained brown in >10% of the cells.

Overexpressed eEF2 gene is a non-mutated, wild-type. To examine whether or not the overexpressed *eEF2* gene was non-mutated, wild-type, the 5' (84-1334 nt) and the 3' (1314-2660 nt) sequences of eEF2 mRNA (coding sequence: 84-2660 nt) from five lung adenocarcinomas and five HNSCCs were amplified by RT-PCR and direct sequencing. No mutation was found in the *eEF2* gene in the 10 cancers examined (data not shown).

Knockdown of eEF2 inhibits cancer cell growth. To examine the role of eEF2 in cancer cell growth, either of two different shRNAs targeting eEF2 (shEF-1918 and shEF-2804) or a control shRNA targeting luciferase (shLuc) was transfected into four eEF2-expressing cells, lung cancer PC14, pancreatic cancer PCI6, fibrosarcoma HT-1080, and glioblastoma A172 and eEF2-undetectable breast cancer MCF7 cells. After culture for 72 h, both of the two shRNAs targeting eEF2 (shEF-1918 and shEF-2804) reduced eEF2 protein expression levels (Fig. 3A) and significantly inhibited cell growth in all the four eEF2-expressing cells examined (Fig. 3B). However, neither of the two shRNAs targeting eEF2 inhibited growth of eEF2-undetectable MCF7 cells.

*Identification of eEF2 peptides that bind to HLA-A*24:02 or HLA-A*02:01 molecules.* Epitope candidates of eEF2 that bound to HLA-A*24:02 or HLA-A*02:01 molecules were first analysed using ProPred-I computer algorithm (Table II).

As candidate epitope peptides that bound to HLA-A*24:02 molecules, EF78, EF786, EF701 and EF412 peptides were selected and analyzed for binding affinity to HLA-A*24:02 molecules by the MHC stabilization assay. These peptides were pulsed to T2-2402 cells and the expression of HLA-A*24:02 molecules on the cell surface was analyzed by flow cytometry. As shown in Table II, all the four peptides increased the expression of HLA-A24:02 molecules on T2-2402 cells as a result of the stabilization of HLA-A24:02 molecules. Among the four peptides, EF786 peptide showed binding affinity higher than $CMVpp65_{328-336}$, which was an exogenous cytomegalovirus antigen epitope, to the HLA-A*24:02 molecules. As candidate peptides that bound to HLA-A*02:01 molecules, EF292, EF739, EF519 and EF671 peptides were selected and analyzed for binding affinity to HLA-A*02:01 molecules by the MHC stabilization assay. As shown in Table II, all the four peptides increased the expression of HLA-A02:01 molecules on T2-0201 cells and EF292 peptide showed the highest binding affinity to HLA-A*02:01 molecules among the four HLA-A*02:01-binding peptides examined.

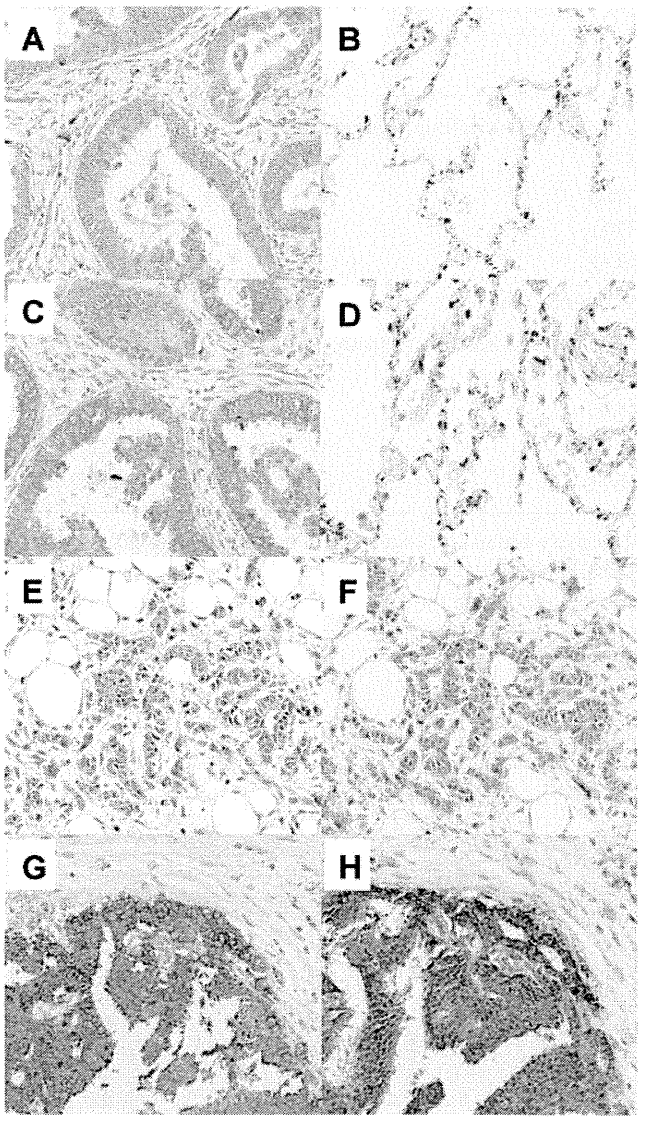

Figure 2. Overexpression of eEF2 in various types of cancers. Representative results of immunohistochemical analysis for eEF2 protein expression in (A and C) lung adenocarcinoma, (B and D) normal lung cells, (E and F) breast cancer, and (G and H) prostate cancer. eEF2 was stained with (A, B, E and G) eEF2-H118 antibody or (C, D, F and H) #SAB4500695 antibody. eEF2 protein was stained brown. Macrophages are non-specifically stained in normal lung tissues.

*Generation of EF2-specific CTLs from HLA-A*24:02- or HLA-A*02:01-positive donors.* Treg-depleted PBMCs from

Table II. Characteristics of EF2-derived peptides and results of the MHC stabilization assay.

Peptide	Position (aa)	Sequence	Score	%MFI increase
HLA-A*24:02-binding peptides				
EF78	78-86	FYELSENDL	360	40.5
EF786	786-794	AYLPVNESF	252	1552.1
EF701	701-709	RFDVHDVTL	40	297.3
EF412	412-420	AFGRVFSGL	33.6	47.9
CMVpp65 328-336		QYDPVAALF		1344.1
HLA-A*02:01-binding peptides				
EF292	292-300	LILDPIFKV	3290	183.3
EF739	739-747	RLMEPIYLV	2426	141.1
EF519	519-527	KLVEGLKRL	705	58.9
EF671	671-679	YLNEIKDSV	642	89.6

The primary amino acid sequences of human eEF2 were analyzed for consensus motifs for 9-mer peptides capable of binding to HLA-A*24:02 or 02:01 molecules using ProPred-I software. Percentage MFI increase in MHC stabilization assay was calculated as follows: percentage MFI increase = (MFI with the given peptide - MFI without peptide)/(MFI without peptide) x 100.

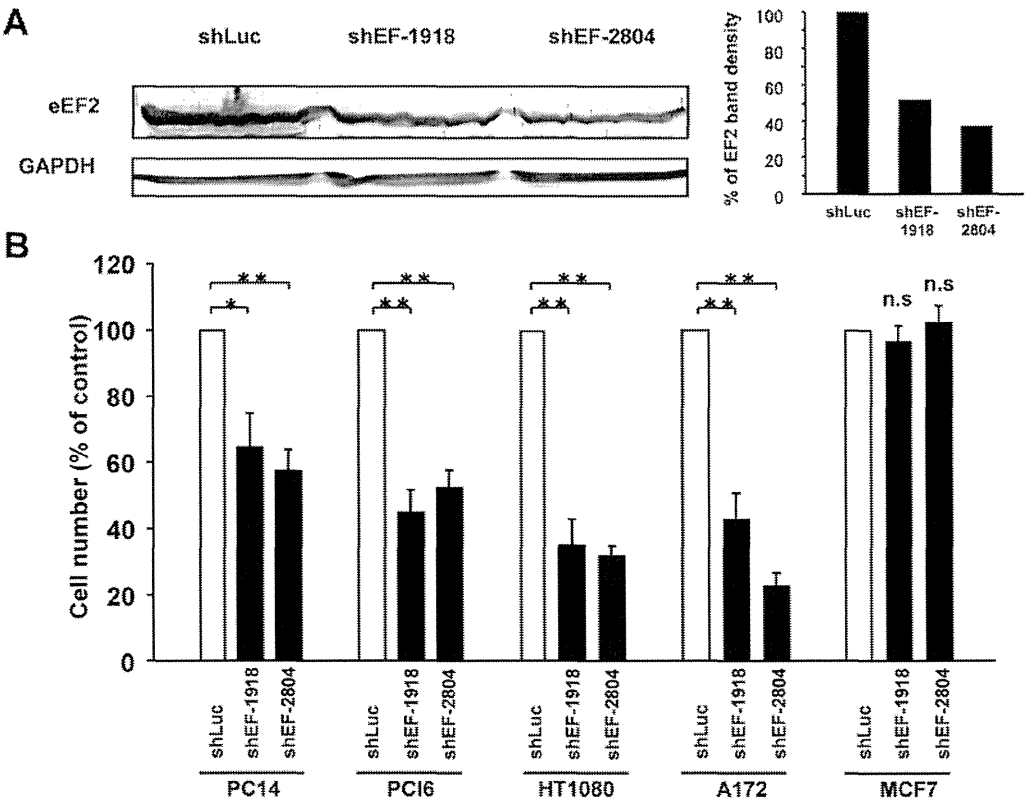

Figure 3. Knockdown of eEF2 inhibits cancer cell growth. Two shRNA vectors targeting different sequences of eEF2 (shEF-1918 and shEF-2804 targeting 1918-1947 and 2804-2833 nt of eEF2 sequence, respectively) or control shRNA targeting luciferase (shLuc) was transfected into PC14, PCI6, HT1080, A172 and MCF7 cells. (A) Reduction in eEF2 protein expression levels in HT1080 cells. Results of western blot analysis are shown. (B) After 72 h of transfection, the cell numbers were examined. *p<0.05; **p<0.01. Experiments were independently performed three times.

HLA-A*24:02- or HLA-A*02:01-positive healthy donors were repeatedly stimulated with EF2 peptides (EF786 and EF292 peptides for HLA-A*24:02- and HLA-A*02:01-positive healthy donors, respectively) and pulsed irradiated autologous DCs and EF2 peptide-specific CTLs were established.

To examine whether EF2 peptides are capable of eliciting CTL responses, CTL activities of established CTLs were examined. As shown in Fig. 4A, EF786-specific, HLA-A*24:02-restricted CTLs lysed EF786 peptide-pulsed T2-2402 cells but not unpulsed ones. The EF786-specific

Table III. Characteristics of target cells in the killing assay.

Target cells	HLA-A*24:02 expression	HLA-A*02:01 expression	eEF2 expression
T2	-	-	Undetectable
T2-2402	+	-	Undetectable
T2-0201	-	+	Undetectable
SW480	+		+
AZ-521	-		+
MKN28	-		+
TF-1		+	+
K562	-	-	+
MCF7		+	Undetectable

Cell surface protein expression of HLA-A molecules was confirmed by flow cytometry. Expression of eEF2 protein was analyzed by western blot analysis.

CTLs lysed HLA-A*24:02-positive, eEF2-expressing SW480 cells, but not HLA-A*24:02-negative, eEF2-expressing AZ-521 and MKN28 cells. As shown in a Fig. 4B, EF292 peptide-specific, HLA-A*02:01-restricted CTLs lysed EF292 peptide-pulsed T2-0201 cells but not unpulsed ones. Moreover, the EF292-specific CTLs lysed HLA-A*02:01-positive, eEF2-expressing TF-1 cells, but not HLA-A*02:01-negative, eEF2-expressing K562 cells and HLA-A*02:01-positive, eEF2-undetectable MCF7 cells (Fig. 4B).

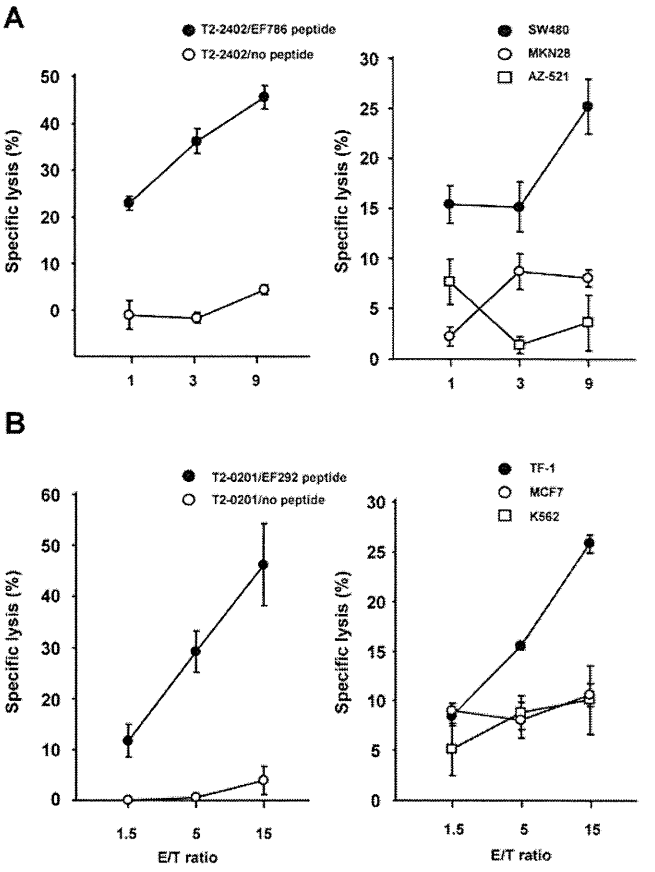

Figure 4. Generation of eEF2-specific CTLs. (A, left panel) Specific lysis of EF786 peptide-pulsed T2-2402 cells by EF786-specific, HLA-A*24:02-restricted CTLs. (A, right panel) Specific lysis of eEF2-expressing, HLA-A*24:02-positive SW480 by EF786-specific, HLA-A*24:02-restricted CTLs. AZ-521 and MKN28 are eEF2-expressing, but HLA-A*24:02-negative. (B, left panel) Specific lysis of EF292 peptide-pulsed T2-0201 cells by EF292-specific, HLA-A*02:01-restricted CTLs. (B, right panel) Specific lysis of eEF2-expressing, HLA-A*02:01-positive TF-1 cells by EF292-specific, HLA-A*02:01-restricted CTLs. K562 is eEF2-expressing and HLA-A*02:01-negative, and MCF7 is eEF2-undetectable and HLA-A*02:01-positive. E/T, effector/target ratio. CTL cytotoxic assays were performed in triplicate.

Discussion

We showed that eEF2 was overexpressed in the majority of various types of tumors such as lung, esophageal, pancreatic, and breast cancer and promoted growth of various types of cancer cells. Moreover, *eEF2* gene product elicited both humoral and cellular eEF2-specific immune responses. The production of eEF2 IgG autoantibody was enhanced in patients with colorectal and gastric cancer and 9-mer eEF2 peptides elicited EF2-specific CTLs from healthy donors. These results indicated that overexpressed eEF2 played an oncogenic role and served as a TAA in these tumors.

It is considered that production of autoantibody indicates the potential of its antigen as a target of cancer immunotherapy (20). In the present study, we showed the elevation of serum EF2 IgG levels in colorectal and gastric cancer patients, indicating that eEF2 overexpressed in cancer cells was recognized by the host immune system and induced eEF2-specific immune responses. Since production of IgG autoantibody needed help from $CD4^+$ helper T cells (Th cells) for class switch from IgM to IgG, elevation of EF2 IgG Ab levels indicated the activation of EF2-specific Th cells. It is well established that Th cells play an important role in the immune responses against cancer (21). $CD4^+$ Th cells are required for activation and maintenance of $CD8^+$ CTLs, but they could also exert cytotoxic function against cancer in the absence of $CD8^+$ CTLs recognizing antigenic peptides presented by MHC class II molecules (22,23). These results indicated that EF2 protein was an immunogenic molecule that is capable of eliciting not only humoral but also cellular immune responses. In fact, eEF2-derived EF786 peptide showed the binding affinity higher than CMVpp65328-336, an exogenous viral antigen epitope, and elicited *in vitro* EF786-specific CTLs from PBMCs of HLA-A*24:02-positive healthy donors. Taken together, eEF2 protein is highly immunogenic and a promising target molecule for cancer immunotherapy.

Expression of target molecules in tumor cells is the first requisite for TAA-targeting cancer immunotherapy. Survivin is a member of the family of the inhibitor of apoptosis proteins and functions as a key regulator of mitosis and programmed cell death (24). Survivin is overexpressed in various types of tumors with the frequency of 34.5% in gastric cancers (25), 50-60% in colorectal cancers (25,26), 64% in malignant gliomas (27), 53-72% in lung cancers (28,29), and 70.7% in breast cancers (30). Cancer vaccines to induce an antigen-specific immune responses against survivin-expressing tumor cells have been developed with

promising results (31,32). Thus, survivin appears to be a promising TAA. However, survivin-targeted immunotherapy may be applicable to a limited population of patients because of its low expression rates in several tumors. In addition, the frequency of survivin-positive tumor cells may vary in individual tumors (25). Thus, the existence of tumor cells lacking survivin could result in tumor evasion from CTL responses against survivin induced by vaccination. NY-ESO-1 is a member of cancer testis antigens and is expressed in a variety of common cancers. Clinical trials that evaluate therapeutic responses against NY-ESO-1 are underway in various cancers (33). However, NY-ESO-1 protein was expressed in only 20 to 30% of lung (34), bladder and ovarian cancers (35) and melanoma and was undetectable in colon and renal cancers (36). Thus, therapeutic strategy against NY-ESO-1 is applicable to a minor population of cancer patients. Compared to these TAAs, eEF2 is more attractive as a target molecule of cancer immunotherapy because of its high frequency of overexpression in various types of cancers. The frequency of eEF2 overexpression exceeded 70% in lung, esophageal, breast and prostate cancers, and 90% in gastric and colorectal cancers and NHL, as shown in the present and previous (14) studies. These results indicated that eEF2-targeted immunotherapy should be a therapeutic strategy that would be applicable to the majority of cancer patients. WT1 is also a promising target molecule of immunotherapy and was ranked as top of TAAs (37). WT1 is overexpressed in the majority of leukemia (38) and various types of tumors such as lung (39), colorectal (40) and pancreatic cancer (41), and glioblastoma multiforme (42). However, WT1 might be less expressed in malignant lymphoma. In diffuse large B-cell lymphoma the most common type of NHL, WT1 protein was detected in only 33% of the cases examined (43). Thus, eEF2-targeted immunotherapy may have a priority for NHL.

One mechanism for escape from immune surveillance is the loss of expression of target molecules in cancer cells (44). Therefore, it is important to know whether or not loss of eEF2 expression affects tumor growth in consideration of the potential of eEF2 as a target molecule for cancer immmunotherapy. As shown in the present study, knockdown of eEF2 by shRNA significantly inhibited cancer cell growth. Also, we have demonstrated that eEF2 was overexpressed in the majority of gastric and colorectal cancers and promoted progression of G_2/M in the cell cycle, resulting in the enhancement of *in vitro* and *in vivo* cancer cell growth (14). Based on these findings showing the involvement of eEF2 in cancer cell growth, it is unlikely that antigenic loss of eEF2 could become a mechanism of tumor escape from eEF2-specific immune responses.

A primary goal of cancer immunotherapy is generation of effective CTL responses through the expansion of robust pre-existing, naturally occurring $CD8^+$ CTL precursors and the establishment of long-lasting memory $CD8^+$ T cells. This critically depends on the activation of pre-existing antigen-specific CTL precursors as the initial step to induce immune responses. In the present study, eEF2-specific CTL clones were established from HLA-A*24:02- or HLA-A*02:01-positive healthy donors. In addition, eEF2 IgG autoantibody is detected at low levels in healthy individuals examined. Since these results indicated the existence of not only eEF2-specific CTL precursors but also eEF2-specific B and Th cells even in healthy donors without cancer, the host immune system of cancer patients should have a potential to make robust immune responses against eEF2-expressing cancers by vaccination with EF2 protein or peptide.

In conclusion, eEF2 that is overexpressed in a wide variety of cancers is a promising cancer antigen that can elicit both humoral and cellular immune responses and shows promise as a target molecule of cancer immunotherapy.

Acknowledgements

We thank Shigemi Norioka (Osaka University) and Mamoru Sato (Chiba University) for their technical support on isoelectric focusing. We also thank Kaori Miyazaki and Atsushi Okumura (Osaka University) for their experimental assistance. This study was supported in part by a Grant-in-Aid from the Ministry of Education, Science, Sports, Culture and Technology, Japan, the Ministry of Health, Labour and Welfare, Japan and Fukui Satoshi Medical Research Foundation.

References

1. Lesterhuis WJ, Haanen JB and Punt CJ: Cancer immunotherapy - revisited. Nat Rev Drug Discov 10: 591-600, 2011.
2. Wright SE: Immunotherapy of breast cancer. Expert Opin Biol Ther 12: 479-490, 2012.
3. Slingluff CL Jr: The present and future of peptide vaccines for cancer: single or multiple, long or short, alone or in combination? Cancer J 17: 343-350, 2011.
4. Murala S, Alli V, Kreisel D, Gelman AE and Krupnick AS: Current status of immunotherapy for the treatment of lung cancer. J Thorac Dis 2: 237-244, 2010.
5. Topalian SL, Weiner GJ and Pardoll DM: Cancer immunotherapy comes of age. J Clin Oncol 29: 4828-4836, 2011.
6. Desmetz C, Mange A, Maudelonde T and Solassol J: Autoantibody signatures: progress and perspectives for early cancer detection. J Cell Mol Med 15: 2013-2024, 2011.
7. Murphy MA, O'Leary JJ and Cahill DJ: Assessment of the humoral immune response to cancer. J Proteomics 75: 4573-4579, 2012.
8. Grzmil M and Hemmings BA: Translation regulation as a therapeutic target in cancer. Cancer Res 72: 3891-3900, 2012.
9. Bilanges B and Stokoe D: Mechanism of translational deregulation in human tumors and therapeutic intervention strategies. Oncogene 26: 5973-5990, 2007.
10. Hizli AA, Chi Y, Swanger J, Carter JH, Liao Y, Welcker M, Ryazanov AG and Clurman BE: Phosphorylation of eukaryotic elongation factor 2 (eEF2) by cyclin A-cyclin-dependent kinase 2 regulates its inhibition by eEF2 kinase. Mol Cell Biol 33: 596-604, 2013.
11. White SJ, Kasman LM, Kelly MM, Lu P, Spruill L, McDermott PJ and Voelkel-Johnson C: Doxorubicin generates a proapoptotic phenotype by phosphorylation of EF-2. Free Radic Biol Med 43: 1313-1321, 2007.
12. Kruiswijk F, Yuniati L, Magliozzi R, Low TY, Lim R, Bolder R, Mohammed S, Proud CG, Heck AJ, Pagano M and Guardavaccaro D: Coupled activation and degradation of eEF2K regulates protein synthesis in response to genotoxic stress. Sci Signal 5: ra40, 2012.
13. Schwer CI, Stoll P, Rospert S, Fitzke E, Schallner N, Burkle H, Schmidt R and Humar M: Carbon monoxide releasing molecule-2 CORM-2 represses global protein synthesis by inhibition of eukaryotic elongation factor eEF2. Int J Biochem Cell Biol 45: 201-212, 2013.
14. Nakamura J, Aoyagi S, Nanchi I, Nakatsuka S, Hirata E, Shibata S, Fukuda M, Yamamoto Y, Fukuda I, Tatsumi N, Ueda T, Fujiki F, Nomura M, Nishida S, Shirakata T, Hosen N, Tsuboi A, Oka Y, Nezu R, Mori M, Doki Y, Aozasa K, Sugiyama H and Oji Y: Overexpression of eukaryotic elongation factor eEF2 in gastrointestinal cancers and its involvement in G_2/M progression in the cell cycle. Int J Oncol 34: 1181-1189, 2009.

15. Kuzushima K, Hayashi N, Kimura H and Tsurumi T: Efficient identification of HLA-A*2402-restricted cytomegalovirus-specific CD8(+) T-cell epitopes by a computer algorithm and an enzyme-linked immunospot assay. Blood 98: 1872-1881, 2001.
16. Oka Y, Elisseeva OA, Tsuboi A, Ogawa H, Tamaki H, Li H, Oji Y, Kim EH, Soma T, Asada M, Ueda K, Maruya E, Saji H, Kishimoto T, Udaka K and Sugiyama H: Human cytotoxic T lymphocyte responses specific for peptides of wild-type Wilms' tumor gene WT1 product. Immunogenetics 51: 99-107, 2000.
17. Masuda T, Ide N and Kitabatake N: Effects of chemical modification of lysine residues on the sweetness of lysozyme. Chem Senses 30: 253-264, 2005.
18. Oji Y, Kitamura Y, Kamino E, Kitano A, Sawabata N, Inoue M, Mori M, Nakatsuka S, Sakaguchi N, Miyazaki K, Nakamura M, Fukuda I, Nakamura J, Tatsumi N, Takakuwa T, Nishida S, Shirakata T, Hosen N, Tsuboi A, Nezu R, Maeda H, Oka Y, Kawase I, Aozasa K, Okumura M, Miyoshi S and Sugiyama H: WT1 IgG antibody for early detection of nonsmall cell lung cancer and as its prognostic factor. Int J Cancer 125: 381-387, 2009.
19. Morishima S, Akatsuka Y, Nawa A, Kondo E, Kiyono T, Torikai H, Nakanishi T, Ito Y, Tsujimura K, Iwata K, Ito K, Kodera Y, Morishima Y, Kuzushima K and Takahashi T: Identification of an HLA-A24- restricted cytotoxic T lymphocyte epitope from human papillomavirus type-16 E6: the combined effects of bortezomib and interferon-gamma on the presentation of a cryptic epitope. Int J Cancer 120: 594-604, 2007.
20. Chiriva-Internati M, Yu Y, Mirandola L, D'Cunha N, Hardwicke F, Cannon MJ, Cobos E and Kast WM: Identification of AKAP-4 as a new cancer/testis antigen for detection and immunotherapy of prostate cancer. Prostate 72: 12-23, 2012.
21. Qin Z and Blankenstein T: CD4+ T cell-mediated tumor rejection involves inhibition of angiogenesis that is dependent on IFNγ receptor expression by nonhematopoietic cells. Immunity 12: 677-686, 2000.
22. Bogen B, Munthe L, Sollien A, Hofgaard P, Omholt H, Dagnaes F, Dembic Z and Lauritzsen GF: Naive CD4+ T cells confer idiotype-specific tumor resistance in the absence of antibodies. Eur J Immunol 25: 3079-3086, 1995.
23. Lin Y, Fujiki F, Katsuhara A, Oka Y, Tsuboi A, Aoyama N, Tanii S, Nakajima H, Tatsumi N, Morimoto S, Tamanaka T, Tachino S, Hosen N, Nishida S, Oji Y, Kumanogoh A and Sugiyama H: HLA-DPB1*05:01-restricted WT1 332-specific TCR-transduced CD4+ T lymphocytes display a helper activity for WT1-specific CTL induction and a cytotoxicity against leukemia cells. J Immunother 36: 159-170, 2013.
24. Mita AC, Mita MM, Nawrocki ST and Giles FJ: Survivin: key regulator of mitosis and apoptosis and novel target for cancer therapeutics. Clin Cancer Res 14: 5000-5005, 2008.
25. Lu CD, Altieri DC and Tanigawa N: Expression of a novel anti-apoptosis gene, survivin, correlated with tumor cell apoptosis and p53 accumulation in gastric carcinomas. Cancer Res 58: 1808-1812, 1998.
26. Kawasaki H, Altieri DC, Lu CD, Toyoda M, Tenjo T and Tanigawa N: Inhibition of apoptosis by survivin predicts shorter survival rates in colorectal cancer. Cancer Res 58: 5071-5074, 1998.
27. Chakravarti A, Noll E, Black PM, Finkelstein DF, Finkelstein DM, Dyson NJ and Loeffler JS: Quantitatively determined survivin expression levels are of prognostic value in human gliomas. J Clin Oncol 20: 1063-1068, 2002.
28. Wang M, Liu BG, Yang ZY, Hong X and Chen GY: Significance of survivin expression: Prognostic value and survival in stage III non-small cell lung cancer. Exp Ther Med 3: 983-988, 2012.
29. Bria E, Visca P, Novelli F, Casini B, Diodoro MG, Perrone-Donnorso R, Botti C, Sperduti I, Facciolo F, Milella M, Cecere FL, Cognetti F and Mottolese M: Nuclear and cytoplasmic cellular distribution of survivin as survival predictor in resected non-small-cell lung cancer. Eur J Surg Oncol 34: 593-598, 2008.
30. Tanaka K, Iwamoto S, Gon G, Nohara T, Iwamoto M and Tanigawa N: Expression of survivin and its relationship to loss of apoptosis in breast carcinomas. Clin Cancer Res 6: 127-134, 2000.
31. Idenoue S, Hirohashi Y, Torigoe T, Sato Y, Tamura Y, Hariu H, Yamamoto M, Kurotaki T, Tsuruma T, Asanuma H, Kanaseki T, Ikeda H, Kashiwagi K, Okazaki M, Sasaki K, Sato T, Ohmura T, Hata F, Yamaguchi K, Hirata K and Sato N: A potent immunogenic general cancer vaccine that targets survivin, an inhibitor of apoptosis proteins. Clin Cancer Res 11: 1474-1482, 2005.
32. Kameshima H, Tsuruma T, Torigoe T, Takahashi A, Hirohashi Y, Tamura Y, Tsukahara T, Ichimiya S, Kanaseki T, Iwayama Y, Sato N and Hirata K: Immunogenic enhancement and clinical effect by type-I interferon of anti-apoptotic protein, survivin-derived peptide vaccine, in advanced colorectal cancer patients. Cancer Sci 102: 1181-1187, 2011.
33. Cebon J, Knights A, Ebert L, Jackson H and Chen W: Evaluation of cellular immune responses in cancer vaccine recipients: lessons from NY-ESO-1. Expert Rev Vaccines 9: 617-629, 2010.
34. Kim SH, Lee S, Lee CH, Lee MK, Kim YD, Shin DH, Choi KU, Kim JY, Park do Y and Sol MY: Expression of cancer-testis antigens MAGE-A3/6 and NY-ESO-1 in non-small-cell lung carcinomas and their relationship with immune cell infiltration. Lung 187: 401-411, 2009.
35. Yakirevich E, Sabo E, Lavie O, Mazareb S, Spagnoli GC and Resnick MB: Expression of the MAGE-A4 and NY-ESO-1 cancer-testis antigens in serous ovarian neoplasms. Clin Cancer Res 9: 6453-6460, 2003.
36. Jungbluth AA, Chen YT, Stockert E, Busam KJ, Kolb D, Iversen K, Coplan K, Williamson B, Altorki N and Old LJ: Immunohistochemical analysis of NY-ESO-1 antigen expression in normal and malignant human tissues. Int J Cancer 92: 856-860, 2001.
37. Cheever MA, Allison JP, Ferris AS, Finn OJ, Hastings BM, Hecht TT, Mellman I, Prindiville SA, Viner JL, Weiner LM and Matrisian LM: The prioritization of cancer antigens: a national cancer institute pilot project for the acceleration of translational research. Clin Cancer Res 15: 5323-5337, 2009.
38. Inoue K, Sugiyama H, Ogawa H, Nakagawa M, Yamagami T, Miwa H, Kita K, Hiraoka A, Masaoka T, Nasu K, Kyo T, Dohy H, Nakauchi H, Ishidate T, Akiyama T and Kishimoto T: WT1 as a new prognostic factor and a new marker for the detection of minimal residual disease in acute leukemia. Blood 84: 3071-3079, 1994.
39. Oji Y, Miyoshi S, Maeda H, Hayashi S, Tamaki H, Nakatsuka S, Yao M, Takahashi E, Nakano Y, Hirabayashi H, Shintani Y, Oka Y, Tsuboi A, Hosen N, Asada M, Fujioka T, Murakami M, Kanato K, Motomura M, Kim EH, Kawakami M, Ikegame K, Ogawa H, Aozasa K, Kawase I and Sugiyama H: Overexpression of the Wilms' tumor gene WT1 in de novo lung cancers. Int J Cancer 100: 297-303, 2002.
40. Oji Y, Yamamoto H, Nomura M, Nakano Y, Ikeba A, Nakatsuka S, Abeno S, Kiyotoh E, Jomgeow T, Sekimoto M, Nezu R, Yoshikawa Y, Inoue Y, Hosen N, Kawakami M, Tsuboi A, Oka Y, Ogawa H, Souda S, Aozasa K, Monden M and Sugiyama H: Overexpression of the Wilms' tumor gene WT1 in colorectal adenocarcinoma. Cancer Sci 94: 712-717, 2003.
41. Oji Y, Nakamori S, Fujikawa M, Nakatsuka S, Yokota A, Tatsumi N, Abeno S, Ikeba A, Takashima S, Tsujie M, Yamamoto H, Sakon M, Nezu R, Kawano K, Nishida S, Ikegame K, Kawakami M, Tsuboi A, Oka Y, Yoshikawa K, Aozasa K, Monden M and Sugiyama H: Overexpression of the Wilms' tumor gene WT1 in pancreatic ductal adenocarcinoma. Cancer Sci 95: 583-587, 2004.
42. Oji Y, Suzuki T, Nakano Y, Maruno M, Nakatsuka S, Jomgeow T, Abeno S, Tatsumi N, Yokota A, Aoyagi S, Nakazawa T, Ito K, Kanato K, Shirakata T, Nishida S, Hosen N, Kawakami M, Tsuboi A, Oka Y, Aozasa K, Yoshimine T and Sugiyama H: Overexpression of the Wilms' tumor gene WT1 in primary astrocytic tumors. Cancer Sci 95: 822-827, 2004.
43. Drakos E, Rassidakis GZ, Tsioli P, Lai R, Jones D and Medeiros LJ: Differential expression of WT1 gene product in non-Hodgkin lymphomas. Appl Immunohistochem Mol Morphol 13: 132-137, 2005.
44. Schreiber RD, Old LJ and Smyth MJ: Cancer immunoediting: integrating immunity's roles in cancer suppression and promotion. Science 331: 1565-1570, 2011.

OPEN ACCESS Freely available online

PLOS | ONE

Profiling the Mitochondrial Proteome of Leber's Hereditary Optic Neuropathy (LHON) in Thailand: Down-Regulation of Bioenergetics and Mitochondrial Protein Quality Control Pathways in Fibroblasts with the 11778G>A Mutation

Aung Win Tun[1], Sakdithep Chaiyarit[2], Supannee Kaewsutthi[1], Wanphen Katanyoo[1], Wanicha Chuenkongkaew[3], Masayoshi Kuwano[4], Takeshi Tomonaga[4], Chayanon Peerapittayamongkol[1], Visith Thongboonkerd[2,5]*, Patcharee Lertrit[1]*

1 Department of Biochemistry, Faculty of Medicine Siriraj Hospital, Mahidol University, Bangkok, Thailand, **2** Medical Proteomics Unit, Office for Research and Development, Faculty of Medicine Siriraj Hospital, Mahidol University, Bangkok, Thailand, **3** Department of Ophthalmology, Faculty of Medicine Siriraj Hospital, Mahidol University, Bangkok, Thailand, **4** Laboratory of Proteome Research, National Institute of Biomedical Innovation, Osaka, Japan, **5** Center for Research in Complex Systems Science, Mahidol University, Bangkok, Thailand

Abstract

Leber's Hereditary Optic Neuropathy (LHON) is one of the commonest mitochondrial diseases. It causes total blindness, and predominantly affects young males. For the disease to develop, it is necessary for an individual to carry one of the primary mtDNA mutations 11778G>A, 14484T>C or 3460G>A. However these mutations are not sufficient to cause disease, and they do not explain the characteristic features of LHON such as the higher prevalence in males, incomplete penetrance, and relatively later age of onset. In order to explore the roles of nuclear encoded mitochondrial proteins in development of LHON, we applied a proteomic approach to samples from affected and unaffected individuals from 3 pedigrees and from 5 unrelated controls. Two-dimensional electrophoresis followed by MS/MS analysis in the mitochondrial lysate identified 17 proteins which were differentially expressed between LHON cases and unrelated controls, and 24 proteins which were differentially expressed between unaffected relatives and unrelated controls. The proteomic data were successfully validated by western blot analysis of 3 selected proteins. All of the proteins identified in the study were mitochondrial proteins and most of them were down regulated in 11778G>A mutant fibroblasts. These proteins included: subunits of OXPHOS enzyme complexes, proteins involved in intermediary metabolic processes, nucleoid related proteins, chaperones, cristae remodelling proteins and an anti-oxidant enzyme. The protein profiles of both the affected and unaffected 11778G>A carriers shared many features which differed from those of unrelated control group, revealing similar proteomic responses to 11778G>A mutation in both affected and unaffected individuals. Differentially expressed proteins revealed two broad groups: a cluster of bioenergetic pathway proteins and a cluster involved in protein quality control system. Defects in these systems are likely to impede the function of retinal ganglion cells, and may lead to the development of LHON in synergy with the primary mtDNA mutation.

Citation: Tun AW, Chaiyarit S, Kaewsutthi S, Katanyoo W, Chuenkongkaew W, et al. (2014) Profiling the Mitochondrial Proteome of Leber's Hereditary Optic Neuropathy (LHON) in Thailand: Down-Regulation of Bioenergetics and Mitochondrial Protein Quality Control Pathways in Fibroblasts with the 11778G>A Mutation. PLoS ONE 9(9): e106779. doi:10.1371/journal.pone.0106779

Editor: Yong-Gang Yao, Kunming Institute of Zoology, Chinese Academy of Sciences, China

Received February 28, 2014; **Accepted** August 8, 2014; **Published** September 12, 2014

Funding: This study was supported by The Thailand Research Fund (http://www.trf.or.th) (BRG518006 to PL and RTA5680004 to VT), Office of the Higher Education Commission (http://www.inter.mua.go.th/main2/index.php) and Mahidol University (http://www.mahidol.ac.th) under the National Research Universities Initiative, and Siriraj Graduate Thesis Scholarship to AWT. The funders had no role in study design, data collection and analysis, decision to publish, or preparation of the manuscript.

Competing Interests: The authors have declared that no competing interests exist.

* Email: patcharee.ler@mahidol.ac.th (PL); thongboonkerd@dr.com (VT)

Introduction

Leber's hereditary optic neuropathy (LHON) [OMIM 535 000] is one of the commonest mitochondrial inherited diseases [1]. It is also one of the common causes of blindness in young men, and more than 80% of LHON patients are male [2]. As a result of degeneration of retinal ganglion cell layers, the patients usually develop bilateral acute or sub-acute, painless loss of central vision [3].

The three missense mitochondrial DNA (mtDNA) mutations 11778G>A, 14484T>C, and 3460G>A are the primary mutations responsible for 95% of LHON cases [4]. These mutations change amino acid R340H, M64V and A52T in ND4, ND6 and ND1 subunits of complex I of mitochondrial OXPHOS respectively. All of the LHON patients detected so far in Thailand carry either 11778G>A (>90% of cases) or 14484T>C [5,6]. Though presence of a primary mutation is necessary to develop the disease, the primary mutations per se cannot explain

the distinctive features of LHON [4,7]. The incomplete penetrance of these mutations, and the disease's greater prevalence in males, imply that carriage of a primary mutation alone is not sufficient to cause pathogenesis, and that additional genetic and environmental factors are involved [4]. Level of heteroplasmy of mutant mtDNA, mtDNA haplogroup, nuclear DNA background and various environmental factors have also been reported to influence the clinical development of LHON [4,8–13]. Many previous studies have been conducted to understand these putative risk factors better, in particular to hunt for nuclear modifier genes. Nuclear genetic analyses have ranged from studies of single genes [14–16] to global gene expression profiling studies [17–19]. Given that both mitochondrial and nuclear genes encode OXPHOS subunits and that there is cross-talk between mitochondria and the nucleus, differential expression of both mitochondrial and nuclear genes is observed in various OXPHOS deficiency models [19]. The mitochondrial proteome contains approximately 1,000 proteins, 99% of which are the products of nuclear genes [20]. The coordinated expressions of imported nuclear encoded proteins with the 13 mtDNA-encoded proteins are crucial for the integrity of mitochondrial function.

In order to search for nuclear encoded mitochondrial proteins that may influence the development of LHON, this study compares the mitochondrial proteomic profiles of fibroblasts from affected and unaffected individuals in LHON families with those of unrelated controls, using 2-Dimensional Polyacrylamide Gel Electrophoresis (2-DE) and mass spectrometry.

Materials and Methods

Patients and Their Unaffected Relatives

The samples employed in this study were cultured dermal fibroblasts, directly obtained from 7 affected LHON patients from 3 unrelated pedigrees, 3 unaffected relatives from the 3 families (one from each), and 5 unrelated controls. All LHON cases were diagnosed by an ophthalmologist (WC) and were confirmed to be homoplasmic carriers of the 11778G>A mtDNA mutation. The 3 unaffected relatives were maternally related to the affected individuals and all of them were homoplasmic carriers of the 11778G>A mtDNA mutation (Figure S1). As a control group, five individuals with no familial history of eye diseases were recruited. They were recruited during visits to Siriraj Hospital, Bangkok, Thailand, for reasons unrelated to eye diseases or chronic metabolic diseases. The study was approved by the Ethics Committee of the Mahidol University, Faculty of Medicine, Siriraj Hospital (No. 161/2551) and the study was conducted according to the principal of the World Medical Association's Declaration of Helsinki. Written informed consent was provided for all the samples used in the research.

Fibroblast Cell Culture

The primary dermal fibroblasts from the affected and unaffected relatives, and the unrelated controls were cultivated and maintained at 37°C with 12% (v/v) fetal bovine serum (FBS) in Dulbecco's modified Eagle's medium supplemented with amphotericin B (1 μg/ml), penicillin (100 U/ml), streptomycin (100 μg/ml), 2 mM L-Glutamine, uridine 50 μg/ml [21] in humidified 5% CO_2 atmosphere at 37°C. The medium was refreshed 3 times a week. Cells were harvested at passage 6 for mitochondrial isolation.

Immunofluorescent Staining for Fibroblast Confirmation

For immunofluorescent staining, the cells were washed three times with PBS and fixed in 3.8% formaldehyde in PBS at room temperature for 10 minutes. After rinsing with PBS, the fixed cells were blocked with 1% BSA PBS for 30 minutes. Mouse monoclonal anti-Fibroblast surface protein (Abcam, Cambridge, USA) (1:50) was incubated for 2 hours at room temperature. After washing with PBS for 3 times, the cells were incubated with secondary antibody (rabbit anti-mouse conjugated with FITC 1:2,000 in 1% BSA PBS) and Hoechst-dye 33342 at a dilution of 1:1,000 at room temperature in the dark. Then, the cells were rinsed with PBS and mounted with anti-phase solution on glass slide and visualized under fluorescent microscopy (Nikon ECLIPSE 80i, Nikon Corp.; Tokyo, Japan).

Fibroblast Mitochondrial Isolation

Fibroblast mitochondria were isolated by differential centrifugation [22]. Before trypsinization, the cultured cells were washed with chilled PBS at least four times to make sure that there was no residual FBS. The cultured fibroblasts were then trypsinized with 0.25% trypsin-EDTA. Samples of 0.5×10^6 cells were suspended in 1 ml of isolation buffer containing 0.25 M sucrose, 10 mM HEPES (pH 7.5) and 0.1 mM EDTA. Cell suspensions were sonicated with a probe sonicator (Bandelin Sonopuls HD 200; Bandelin electronic; Berlin, Germany) at MS 72/D (50 cycles) for 10 sec. Cell lysates were then centrifuged twice at 1,000 *g* for 10 min to remove cell debris and intact cells, if present. Supernatant was collected and centrifuged at 20,000 *g* for 30 min. Pellets were saved and washed with the buffer containing 0.25 M sucrose and 10 mM HEPES (pH 7.5) and centrifuged again at 20,000 *g* for 20 min. As a final step, the mitochondrial pellets were washed with PBS and centrifuged at 20,000 *g* for 10 min. The whole extraction procedure was performed at 4°C. The mitochondrial pellets were lyzed by Laemmli or 2-DE buffer depending on the subsequent step of the experiment, and the lyzed mitochondrial fractions were kept at −20°C until use.

Mitochondrial Fraction Purity Evaluation

To confirm the purity of the extracted mitochondrial fractions, mitochondrial proteins and the proteins from the whole cell lysate were resolved by western blot analysis, using mitochondrial- and other organelle-specific markers. The mitochondrial pellets or the primary fibroblasts subsequently used for the Western Blot experiments were lyzed by 2x Laemmli buffer containing 4% SDS, 10% 2-mercaptoehtanol, 20% glycerol, and 0.125 M Tris HCl without bromophenol blue [23]. The protein samples were boiled for 5 min at 95°C. In each western blot analysis, 20 μg of total proteins from each sample were loaded. The proteins were resolved by 3.7% SDS-PAGE (stacking gel) and 12% SDS-PAGE (resolving gel) at 150 V for two and a half hours by vertical gel electrophoresis. The resolved proteins in the gel were then electrotransferred to nitrocellulose membrane using a semidry transfer method (Bio-Rad; Hercules, CA) for 80 min with a constant current of 75 mA. Non-specific binding to the membrane was blocked with 5% skimmed milk in PBS for 1 hr. The blocked membranes were probed with the desired specific primary antibodies in 1% skimmed milk or 1% Bovine Serum Albumin in PBS for overnight at 4°C at concentrations according to manufacturers' instructions. Membranes were washed with PBS for 3 times (5 min per wash) and further incubated with the required secondary antibodies conjugated with horse radish peroxidase (Dako, Glostrup, Denmark), in 1% skimmed milk in PBS or 1% BSA in PBS. Incubations with the secondary antibodies were carried out at room temperature for 1 hr, with the concentrations of the secondary antibodies half of those used for the primary antibodies. Bands were visualized by Super Signal West Pico chemiluminescence substrate (Pierce Biotechnology

Table 1. Characteristics of LHON cases and unaffected relatives recruited in the study.

Subjects	Gender	Age at present (years)	Age of onset (years)	Age at skin biopsy (years)	Fibroblast Passage *used*	G11778A	Haplogroup	mtDNA/nDNAratio*	References
Affected LHON									
Pedigree F1									[13,27]
(A1)	M	25	7	20	P6	homoplasmy	M7b1a1e1	0.84	
(A2)	M	26	14	21	P6	homoplasmy	M7b1a1e1	0.79	
Pedigree F9									[13,27]
(A3)	M	30	9	24	P6	homoplasmy	C7a1	0.82	
(A4)	M	49	12	43	P6	homoplasmy	C7a1	0.85	
Pedigree F66									[9]
(A5)	M	42	36	36	P6	homoplasmy	M13c	0.85	
(A6)	M	37	18	33	P6	homoplasmy	M13c	0.68	
(A7)	M	54	20	50	P6	homoplasmy	M13c	0.85	
Unaffected LHON									
Pedigree F1 (U1)	M	30		25	P6	homoplasmy	M7b1a1e1	0.72	[13,27]
Pedigree F9 (U2)	M	21		15	P6	homoplasmy	C7a1	0.47	[13,27]
Pedigree F66 (U3)	F	49		45	P6	homoplasmy	M13c	0.66	[9]
Controls									
C1	M	43		37	P6	NO		0.51	
C2	M	26		20	P6	NO		0.51	
C3	F	46		40	P6	NO		0.66	
C4	F	52		46	P6	NO		0.74	
C5	M	58		52	P6	NO		0.65	

*MtDNA/nuclear DNA from fibroblast of each individual was measured according to Pejznochova M, 2008 [62] by amplification of *ND5* gene in mitochondrial genome from position 13466–13650 (GenBank sequence NC_012920 gi:251831106), and *PARL* gene from nuclear genome from 16912–17165 (GenBank sequence: NC_000003.12 gi:224589815). Real-time PCR amplification was performed on Bio-Rad CFX 96 thermo cycler and the threshold cycle (Ct) was obtained. MtDNA/nuclear DNA ratio was calculated from the Ct (mtDNA)/Ct (nDNA) ratio. The increasing ratio shows decrease in amount of mtDNA per cell [62].

doi:10.1371/journal.pone.0106779.t001

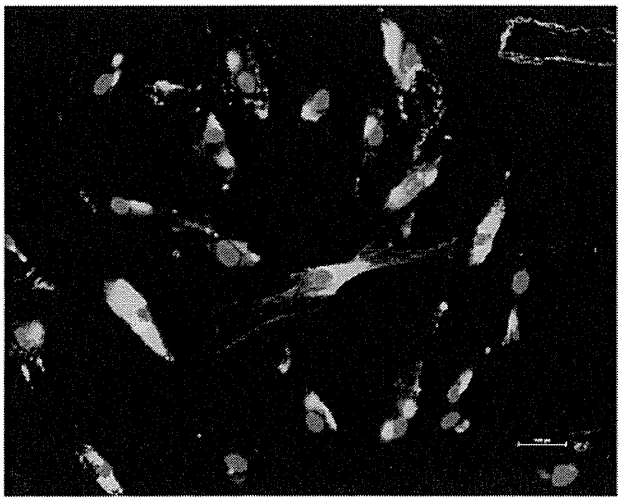

Figure 1. Assessment of the purity of fibroblasts from a cultured skin biopsy. Fibroblast surface protein (FSP) was used as a marker in immunofluorescence of the cultured fibroblasts obtained directly obtained from the skin biopsy. The green represents fibroblasts and the nucleus was stained with Hoechst-dye 33342 which shows blue.
doi:10.1371/journal.pone.0106779.g001

Inc.; Rockford, IL, USA). The following primary antibodies were used: rabbit polyclonal anti-voltage dependent anion selective channel protein 1 (VDAC-1), a mitochondrial marker (Abcam, Cambridge, USA; ab28777); rabbit polyclonal anti-lysosomal associated membrane protein-2 (LAMP-2), a lysosomal marker (Abcam, Cambridge, USA; ab37024); rabbit polyclonal anti-Calnexin, an endoplasmic reticulum marker (Abcam, Cambridge, USA; ab22595); mouse monoclonal anti-c-Jun, a nuclear marker (Santa Cruz Biotechnology, Inc, sc166540) and mouse monoclonal anti-α-tubulin, a cytoplasmic marker (Santa Cruz Biotechnology, Inc, sc23948).

Mitochondrial Proteomics Profile Analyses

Two-Dimensional Electrophoresis. Mitochondrial pellets derived from cultured primary fibroblasts of the 7 individuals with LHON, the 3 unaffected relatives and the five unrelated controls were lyzed with a lysis buffer containing 7 M urea, 2 M thiourea, 2% CHAPS, 120 mM DTT, 40 mM Tris, and 2% ampholyte (pH 3–10), then incubated at 4°C for 30 min. Protein concentration was determined by the Bradford method [24]. Samples of 100 µg of total mitochondrial protein from each individual were mixed with rehydration buffer (7 M urea, 2 M thiourea, 2% CHAPS, 120 mM DTT, 40 mM Tris-base, 2% ampholytes (pH 3–10) and a trace of bromophenol blue) to make the final volume of 150 µl. The samples were rehydrated onto 7 cm immobilized pH gradient DryStrips (non-linear pH gradient of 3–10; GE Healthcare, Uppsala, Sweden) at room temperature for 16 hr. IPG strips were focused in an Ettan IPGphor II IEF System (GE health care) at 20°C using a stepwise mode to reach 9083 Vh.

After isoelectric focusing, the strips were equilibrated in two different equilibration buffers at room temperature, for 15 min each time. The first equilibration buffer contained 6 M urea, 130 mM DTT, 112 mM Tris-base, 4% SDS, 30% glycerol, and 0.002% bromophenol blue, and the second equilibration buffer contained the same components except 135 mM iodoacetamide instead of DTT. The strips were further loaded on 13% polyacrylamide gel and resolved using a SE260 mini Vertical Electrophoresis Unit (GE Health Care) at 150 V for approximately 2 hr. The separated proteins were fixed with 10% methanol and 7% acetic acid for 30 min. The fixed solution was then removed and the gels were stained with 20 ml of Deep Purple fluorescence stain (GE Healthcare) overnight on a continuous gentle rocker. Gel images were taken using a Typhoon 9200 laser scanner (GE Healthcare).

Analysis of Protein Spots. Detection and matching of spots on gel images and analysis of protein spots was performed using ImageMaster 2D Platinum software from GE Health care. Parameters used for spot detection were: minimal area of 10 pixels, smooth factor of 2 and saliency of 2. The gel containing all of the spots and with the greatest number of spots of all the gels was classed as the reference gel. It was used to check for the presence and differential expression of proteins among gels. Background subtraction was performed, and the intensity volume of each spot was normalized with total intensity volume (summation of the intensity volumes obtained from all spots within the same 2-D gel). Intensity volumes of individual spots

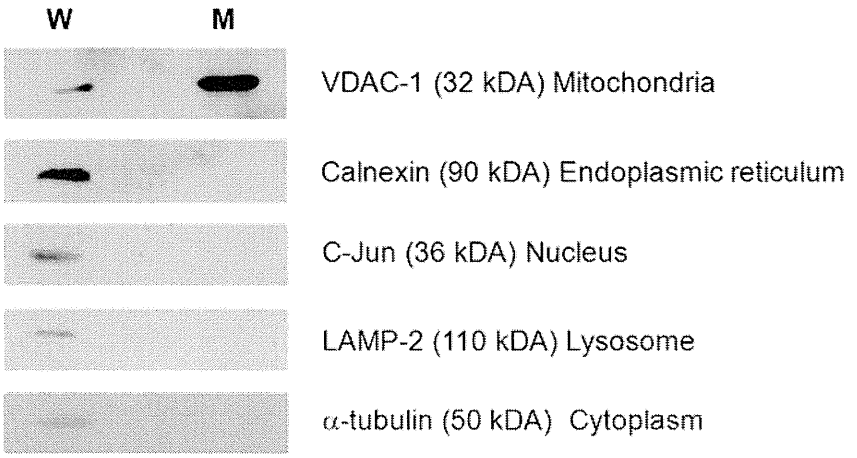

Figure 2. Western blot analyses for assessment of mitochondrial enrichment and purity. 20 µg of mitochondrial lysate and whole cell lysate from fibroblasts were separated by 12% SDS-PAGE gel and checked with specific antibodies against various sub-cellular organelles. (W = whole cell lysate; M = mitochondrial enriched fraction) (The same membrane for each cell type was stripped and probed with subsequent antibodies.).
doi:10.1371/journal.pone.0106779.g002

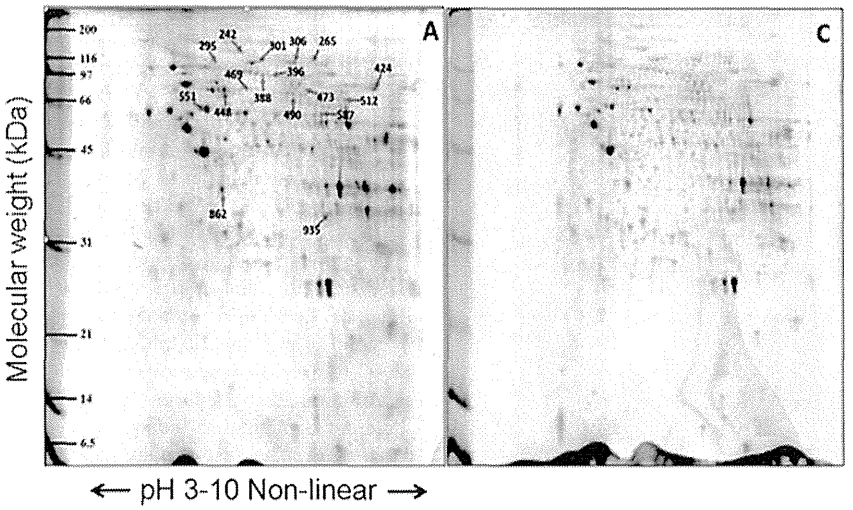

Figure 3. Representative proteome map of differentially expressed proteins from the mitochondrial fractions of fibroblasts from (A) LHON cases (n = 7) and (C) controls (n = 5). Equal amounts of proteins (100 μg) from each fibroblast sample were resolved by 2-DE. The numbers indicate the spot IDs of proteins whose expression levels differ significantly between the fibroblasts of LHON cases and controls.
doi:10.1371/journal.pone.0106779.g003

from each gel were subjected to statistical analysis to compare between the three groups of samples in the study. Protein spots that were differentially expressed at significant levels were subjected to in-gel tryptic digestion for identification by mass spectrometry.

The significantly differentially expressed spots of proteins were manually excised from the gels. The excised gel pieces were washed twice with 200 μL of 50% acetonitrile (ACN)/25 mM NH_4HCO_3 buffer (pH 8.0) at room temperature for 15 min, and then washed once with 200 μL of 100% ACN. After washing, the solvent was removed and the gel pieces were dried. The dried gel plugs were then rehydrated with 10 μL of 1% (w/v) trypsin in 25 mM NH_4HCO_3. After rehydration at 37°C for 30 min, the gel pieces were crushed and further incubated with 1% (w/v) trypsin at 37°C for at least 16 hr. Peptides were subsequently extracted twice with 50 μL of 50% ACN/5% trifluoroacetic acid; the extracted solutions were then combined and dried with the SpeedVac concentrator. The peptide pellets were resuspended with 10 μL of 0.1% TFA and concentrated. The peptide solution was then washed with 10 μL of 0.1% formic acid by drawing up and expelling the washing solution three times. The peptides were eluted with 5 μL of 75% ACN/0.1% formic acid.

Protein Identification by Mass Spectrometry (Q-TOF MS and/or MS/MS). Digested peptides were injected into a Magic C18 column (Michrom Bioresources, Inc., CA, USA), which was connected to the MAGIC 2002 (Michrom Bioresources, Inc., CA, USA) high-performance liquid chromatography (HPLC) system. The solvent composition of the mobile phase was programmed to

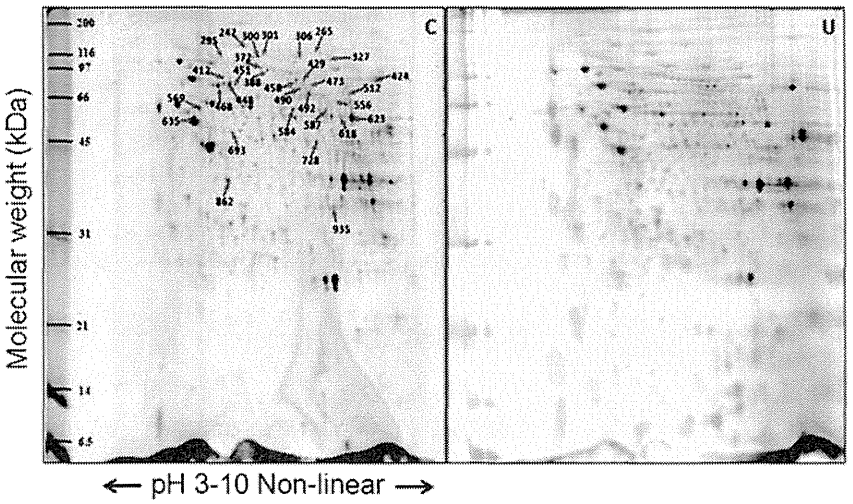

Figure 4. Representative proteome map of differentially expressed proteins from mitochondria fraction between fibroblasts from (U) the unaffected LHON individuals (n = 3) and (C) the controls (n = 5). Equal amounts of proteins (100 μg) from each sample were resolved by 2-DE. The numbers indicate the spot IDs of proteins whose expression levels differ significantly between the fibroblasts of unaffected LHON individuals and controls. Some spots in the same horizontal row showed the same proteins. For example, spot IDs 300 and 301 were identified as LONP1 and IDs 448, 451, 468 as catalase.
doi:10.1371/journal.pone.0106779.g004

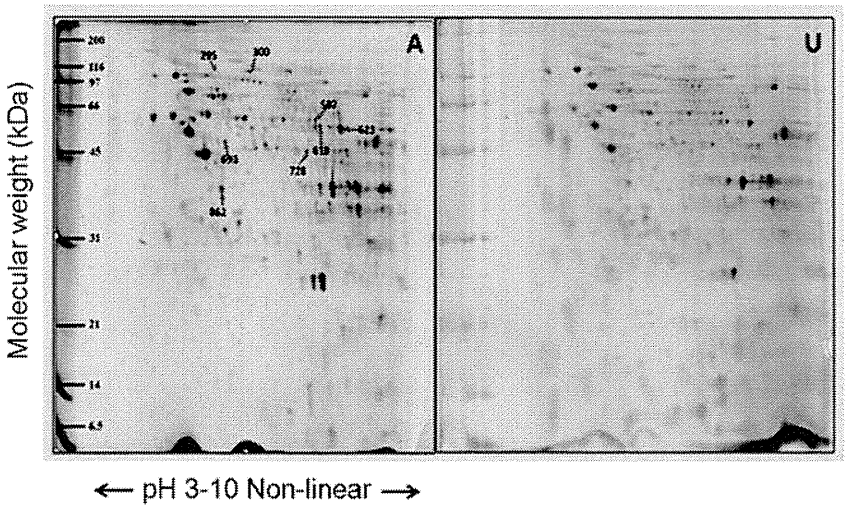

Figure 5. Representative proteome map of differentially expressed proteins from the mitochondrial fractions of fibroblasts from (A) LHON cases (n = 7) and (U) unaffected LHON individuals (n = 3). Equal amounts of proteins (100 μg) from each sample were resolved by 2-DE. The numbers indicate the spot IDs of proteins whose expression levels differ significantly between the LHON cases and their unaffected relatives.
doi:10.1371/journal.pone.0106779.g005

change in 50-min cycles with varying mixing ratios of solvent A (2% v/v CH_3CN and 0.1% v/v HCOOH) to solvent B (90% v/v CH_3CN and 0.1% v/v HCOOH) at flow rate of 1 μL/min using a MAGIC Variable Splitter. Thereafter, the peptides were eluted with a linear gradient from 0% to 50% solvent B. Purified peptides were introduced from HPLC to Q-star (Applied Biosystems, Foster City, CA, USA), a hybrid quadrupole time-of-flight mass spectrometer, through a FortisTip (AMR, Tokyo, Japan). The MS/MS data were extracted and proteins were identified using the MASCOT search engine (http://www.matrixscience.com), assuming that peptides were monoisotopic, and that fixed modifications were carbamidomethylations of cysteine residues, whereas variable modifications were oxidations at methionine residues. Only one missed trypsin cleavage was allowed, and peptide mass tolerances of 50 ppm were allowed for MS/MS ion searches. The searches were done against human proteins in the NCBI database (http://www.ncbi.nlm.nih.gov). Peptides with ion scores greater than 34 were considered as significant hits. Only the significant hits from the MS/MS peptide ion search were reported.

Western Blot Analysis for confirmation of 2-D proteomic results

Western blot analysis was performed to validate the levels of protein expression changes identified in the proteomics profiling. 20 μg samples of the mitochondrial fractions from each sample were resolved employing the same protocol described above. Three primary antibodies were used: rabbit polyclonal HSP60 (Santa Cruz Biotechnology, Inc, sc13966), rabbit polyclonal anti-Catalase (Abcam, Cambridge, USA; ab16731) and rabbit polyclonal NDUFS1 (Abcam, Cambridge, USA; ab96428). Rabbit polyclonal anti-VDAC was used as a loading control. After incubating with the respective secondary antibodies (anti-rabbit), bands were visualized by enhanced chemiluminescence and exposed to film. The band intensities were measured using ImageJ software (http://rsbweb.nih.gov/ij/).

Statistical Analysis

All data representing the intensity volume of the spots were reported as mean ±SEM. For comparison between 3 different groups, the data were analyzed using one-way ANOVA followed by a Post Hoc Tukey-Kramer Test (SPSS, version 18). *P*-values less than 0.05 were considered statistically significant. The false discovery rate (FDR) was determined using R statistical packages for calculating q-values and FDR-values [25,26].

Results

LHON Patients and Their Unaffected Relatives

Samples from individuals in three unrelated LHON pedigrees with different mtDNA haplogroup backgrounds were employed in this study (Figure S1). The numbers of affected LHON patients recruited from pedigrees F1, F9 and F66 were two, two and three respectively. All affected individuals have been diagnosed by an ophthalmologist (WC) and have been confirmed as bearing homoplasmic mtDNA 11778G>A [9,13,27]. The characteristics of each patient are summarized in Table 1. The 3 unaffected relatives came from the 3 pedigrees and were maternally related to the affected individuals and also confirmed to be homoplasmic carriers of the mtDNA 11778G>A mutation. The 11778G>A mutation was not detected in the 5 control individuals recruited in this study, after performing both RFLP genotyping and Sanger sequencing in both the forward and reverse directions.

Confirmation of the purity of Fibroblasts

One of the fibroblast cultures from each of the skin biopsies was randomly selected and tested with anti-fibroblast surface protein which is specific to fibroblasts [28]. Figure 1 shows the results of this immunofluorescent staining with DNA staining Hoechst-dye 33342, which indicated that almost every stained cell had a positive signal for fibroblast surface protein. This confirmed that the fibroblast cultures were pure and uncontaminated by other cell types.

Table 2. Summary of significantly altered proteins between the LHON cases and the control group.

Spot ID	Protein name	Gene*	NCBI ID	Identification scores (MS/MS)	%Cov (MS/MS)	number of matched peptides (MS/MS)	emPAI	p/	MW (kDa)	Intensity (Mean ± SEM)		Fold change Affected/Control	$P^{\#}$	FDR
										Affected (n = 7)	Control (n = 5)			
242	*Leucine-rich PPR motif-containing protein*	LRPPRC	*gi|31621305*	1341	54	72	2.22	5.81	159.00	0.0984±0.0104	0.1746±0.0225	0.48	0.008	0.009
295	Major vault protein	MVP	gi|19913410	743	46	41	1.68	5.34	99.55	0.0519±0.0043	0.0856±0.0062	0.61	0.001	0.003
301	Lon protease homolog	LONP1	gi|21396489	1087	50	50	2.53	6.01	106.94	0.0414±0.0054	0.0861±0.0063	0.48	<0.001	<0.003
306	Vinculin isoform VCL	VCL	gi|4507877	1361	59	64	4.01	5.83	117.22	0.1089±0.0068	0.1704±0.0182	0.64	0.005	0.007
388	Transmembrane protein – mitofilin	IMMT	gi|1160963	1174	67	57	5.97	6.15	83.89	0.1586±0.0121	0.2506±0.0168	0.63	0.001	0.003
396	Methylmalonyl-CoA mutase	MUT	gi|187452	522	34	21	1	6.48	83.54	0.0516±0.0051	0.0843±0.0069	0.61	0.012	0.010
424	Trifunctional enzyme subunit alpha	HADHA	gi|20127408	1297	65	55	4.41	9.16	83.69	0.6631±0.0725	1.0434±0.1170	0.64	0.048	0.0232
448	MTHSP75	HSPA9	gi|292059	2174	68	84	11.1	5.97	74.02	0.4530±0.0536	0.7416±0.1002	0.61	0.030	0.017
469	Cellular myosin heavy chain	MYH9	gi|553596	604	24	25	0.6	5.70	155.29	0.0815±0.0054	0.1414±0.0260	0.58	0.041	0.021
473	Glycerol-3-phosphate dehydrogenase	GPD2	gi|1020315	1080	64	47	3.98	7.58	81.30	0.0341±0.0052	0.0660±0.0100	0.52	0.018	0.013
490	Succinate dehydrogenase [ubiquinone] flavoprotein subunit	SDHA	gi|156416003	1019	57	39	2.96	7.06	73.67	0.1323±0.0105	0.2242±0.0338	0.59	0.018	0.013
512	Very long-chain specific acyl-CoA dehydrogenase	ACADVL	gi|4557235	963	64	38	4.14	8.92	70.35	0.0898±0.0129	0.1423±0.0096	0.63	0.018	0.013
551	60 kDa heat shock protein	HSPD1	gi|31542947	2360	77	99	14.12	5.7	61.19	0.6804±0.5417	0.9936±0.0941	0.68	0.037	0.020
556	Catalase	CAT	gi|4557014	694	55	25	2.54	6.9	59.95	0.0648±0.0095	0.1004±0.0062	0.65	0.025	0.015

Table 2. Cont.

Spot ID	Protein name	Gene*	NCBI ID	Identification scores (MS/MS)	%Cov (MS/MS)	number of matched peptides (MS/MS)	emPAI	p/	MW (kDa)	Intensity (Mean ± SEM)		Fold change Affected/Control	$P^{\#}$	FDR
										Affected (n = 7)	Control (n = 5)			
587	Dihydrolipoamide Dehydrogenase And Dihydrolipoamide Dehydrogenase-Binding Protein (Didomain) Subcomplex Of Human Pyruvate Dehydrogenase Complex.	DLD	gi|83753870	563	51	28	2.86	7.95	54.18	0.1873±0.0124	0.2402±0.0184	0.78	0.047	0.023
862	Pyruvate dehydro-genase E1 component subunit alpha	PDHA1	gi|33357460	572	36	17	1.87	8.35	43.30	0.6067±0.0425	0.7545±0.0185	0.80	0.039	0.020
935	Electron transfer flavoprotein subunit alpha, mitochondrial isoform a	ETFA	gi|4503607	343	63	17	3.47	8.62	33.42	0.2686±0.0210	0.3711±0.0162	0.72	0.007	0.008

*Gene name according to HUGO Gene Nomenclature Committee.
#indicates *P* value based on Post Hoc Tukey Test after one way ANOVA and the value less than 0.05 is considered significant in both tests.
doi:10.1371/journal.pone.0106779.t002

Table 3. Summary of significantly altered proteins between the unaffected LHON individuals and the control group.

Spot ID	Protein name	Gene*	NCBI ID	Identification scores (MS/MS)	%Cov (MS/MS)	number of matched peptides (MS/MS)	emPAI	p/	MW (kDa)	Intensity (Mean ± SEM)		Fold Change	$P^{\neq}$	FDR
										Unaffected (n = 3)	Control (n = 5)	Unaffected/control		
242	*Leucine-rich* PPR motif-containing protein	LRPPRC	*gi|31621305*	1341	54	72	2.22	5.81	159.00	0.0832±0.0076	0.1746±0.0225	0.48	.010	0.009
265	2–Oxoglutarate dehydrogenase	OGDH	gi|51873036	1061	48	51	1.96	6.39	115.94	0.0228±0.0041	0.0769±0.0152	0.30	.033	0.018
295	Major vault protein	MVP	gi|19913410	743	46	41	1.68	5.34	99.55	0.0273±0.0069	0.0856±0.0062	0.32	.000	0.001
300	Lon protease homolog	LONP1	gi|21396489	1004	44	45	2.17	6.01	106.94	0.1572±0.0320	0.3181±0.0222	0.49	.023	0.015
301	Lon protease homolog	LONP1	gi|21396489	1087	50	50	2.53	6.01	106.94	0.0292±0.0055	0.0861±0.0063	0.34	.000	0.002
306	Vinculin isoform VCL	VCL	gi|4507877	1361	59	64	4.01	5.83	117.22	0.0700±0.0014	0.1704±0.0182	0.41	.001	0.003
327	Glucosidase 2 subunit beta isoform 2	PRKCSH	gi|194382324	522	32	22	1.73	4.35	61.07	0.0588±0.0127	0.1365±0.0117	0.43	.018	0.013
372	Mitochondrial inner membrane protein isoform 1	IMMT	gi|154354964	1243	67	50	3.93	6.08	84.03	0.1115±0.0020	0.1752±0.0121	0.64	.008	0.009
388	Transmembrane protein – mitofilin	IMMT	gi|1160963	1174	67	57	5.97	6.15	83.89	0.1312±0.0129	0.2506±0.0168	0.52	.001	0.003
412	NADH dehydrogenase (ubiquinone) Fe-S protein 1	NDUFS1	gi|21411235	1422	63	52	4.55	5.8	80.42	0.1077±0.0112	0.2194±0.0221	0.49	.023	0.015
424	Trifunctional enzyme subunit alpha	HADHA	gi|20127408	1297	65	55	4.41	9.16	83.69	0.4438±0.1842	1.0434±0.1170	0.43	.013	0.011
429	Mitochondrial inner membrane protein isoform 2	IMMT	gi|154354962	1079	66	57	5.69	6.15	83.90	0.1016±0.0099	0.2454±0.0421	0.41	.039	0.020
448	MTHSP75	HSPA9	gi|292059	2174	68	84	11.1	5.97	74.02	0.3171±0.0471	0.7416±0.1002	0.43	.012	0.010
451	MTHSP75	HSPA9	gi|292059	1347	60	57	6.42	5.97	74.02	0.1279±0.0204	0.2277±0.0045	0.56	.024	0.015
458	Propionyl-CoA carboxylase	PCCA	gi|296366	238	23	16	0.26	7.24	80.64	0.0326±0.0031	0.0723±0.0113	0.45	.051	0.024
468	MTHSP75	HSPA9	gi|292059	1068	58	44	4.02	5.97	74.02	0.1996±0.0133	0.4933±0.0143	0.40	.010	0.009
473	*Glycerol-3-* Phosphate dehydrogenase	GPD2	*gi|1020315*	1080	64	47	3.98	7.58	81.30	0.0251±0.0059	0.0660±0.0100	0.38	.015	0.012

Table 3. Cont.

Spot ID	Protein name	Gene*	NCBI ID	Identification scores (MS/MS)	%Cov (MS/MS)	number of matched peptides (MS/MS)	emPAI	p/	MW (kDa)	Intensity (Mean ± SEM)		Fold Change	p≠	FDR
										Unaffected (n = 3)	Control (n = 5)	Unaffected/control		
490	Succinate Dehydrogenase [ubiquinone] Flavoprotein subunit	SDHA	gi|156416003	1019	57	39	2.96	7.06	73.67	0.0628+0.0101	0.2242±0.0338	0.28	.002	0.004
492	Glutaminase kidney isoform	GLS2	gi|156104878	526	42	26	1.65	7.85	74.24	0.0210±0.0055	0.0683±0.0134	0.31	.021	0.014
512	Very long-chain specific acyl-CoA dehydrogenase	ACADVL	gi|4557235	963	64	38	4.14	8.92	70.35	0.0609±0.0078	0.1423±0.0096	0.43	.004	0.006
556	Catalase	CAT	gi|4557014	694	55	25	2.54	6.9	59.95	0.0456±0.0057	0.1004±0.0062	0.45	.007	0.008
569	Vimentin	VIM	gi|62414289	1142	67	49	9.47	5.05	53.68	0.3070±0.0379	0.6188±0.0544	0.50	.015	0.012
584	Glutaminase kidney isoform	GLS2	gi|114582297	1015	55	40	3.86	8.09	66.22	0.155±0.0134	0.3116±0.0314	0.50	.004	0.006
587	Dihydrolipoamide Dehydrogenase And Dihydrolipoamide Dehydrogenase-Binding Protein (Didomain) Subcomplex Of Human Pyruvate Dehydrogenase Complex.	DLD	gi|83753870	563	51	28	2.86	7.95	54.18	0.1219±0.0050	0.2402±0.0184	0.51	.001	0.003
618	Glutamate Dehydrogenase-Apo Form	GLUD1	gi|20151189	743	65	40	5.02	7.66	56.32	0.1841±0.0300	0.3760±0.0191	0.49	.010	0.009
623	ATP synthase subunit alpha	ATP5A1	gi|4757810	1379	65	79	7.26	9.07	59.67	0.5828±0.1452	1.1951±0.0176	0.49	.003	0.004
635	Oxidized Beta-Actin	ACTB	gi|146386601	1118	76	82	14.45	5.29	42.00	0.9409±0.0640	1.8908±0.0496	0.50	.030	0.017
693	Ubiquinol-cytochrome c reductase core I protein	UQCRC1	gi|515634	382	52	22	2.38	5.94	52.59	0.1595±0.0194	0.2847±0.0288	0.56	.009	0.009
728	Ubiquinol-cytochrome c reductase core I protein	UQCRC1	gi|515634	824	48	22	1.76	5.94	53.27	0.1948±0.0222	0.4530±0.0278	0.43	<.001	0.002

Table 3. Cont.

Spot ID	Protein name	Gene*	NCBI ID	Identification scores (MS/MS)	%Cov (MS/MS)	number of matched peptides (MS/MS)	emPAI	p/	MW (kDa)	Intensity (Mean ± SEM)		Fold Change	$p^{\#}$	FDR
										Unaffected (n = 3)	Control (n = 5)	Unaffected/control		
862	Pyruvate Dehydrogenase E1 component subunit alpha	PDHA1	gi|33357460	572	36	17	1.87	8.35	43.30	0.3537±0.0487	0.7545±0.0185	0.47	<.001	0.001
935	Electron transfer Flavoprotein subunit alpha	ETFA	gi|4503607	343	63	17	3.47	8.62	33.42	0.2122±0.0209	0.3711±0.0162	0.57	.002	0.004

*Gene name according to HUGO Gene Nomenclature Committee.

#indicates *P* value based on Post Hoc Tukey Test after one way ANOVA and the value less than 0.05 is considered significant in both tests.

doi:10.1371/journal.pone.0106779.t003

Mitochondrial enrichment and purity

Enrichment and purity of the mitochondrial fraction was assessed by immunoblotting, using markers specific for mitochondria and other organelles. Figure 2 demonstrates that the mitochondrial marker VDAC-1 was highly enriched in the mitochondrial fraction compared with the whole primary fibroblast lysates. In addition, the markers for endoplasmic reticulum, nucleus, lysosome and cytosol were absent or minimal in the mitochondrial enriched fraction. The mitochondrial fraction was highly enriched and with minimal level of non-mitochondrial contamination, and hence it was suitable for further analysis with 2-DE.

Mitochondrial Proteomics Profile Analyses

2-D PAGE comparisons of mitochondrial fraction between fibroblasts from LHON cases, unaffected relatives and unrelated controls. The proteins from the mitochondrial enriched fraction of the primary fibroblasts were analyzed by 2-DE using pH 3–11 non-linear pH gradient strips for the first dimension and 13% SDS-PAGE for the second dimension. The individual 2-D mitochondrial proteome profiles from fibroblasts of individuals with LHON (n = 7), unaffected relatives (n = 3) and unrelated controls (n = 5) showed virtually identical spot patterns (Figure 3, 4 and 5). Approximately 800 protein spots were visualized on each gel. However, spot matching analysis revealed distinct differences in the proteomic profiles of the three groups of samples.

Interestingly, the majority of all differential-intensity spots were lower intensity in the LHON cases than in the unrelated controls. The degrees of fold-change between the cases and the unrelated controls ranged from 0.47 to 2.05. Meanwhile, the fold-changes between the unaffected relatives and the unrelated controls ranged from 0.28 to 3.90, and those between cases and unaffected relatives ranged from 1.5 to 2.2 fold. In total 61 differential intensity spots were identified in the three pairwise comparisons. These were excised from the gels, and their corresponding proteins were identified by MS or MS/MS analysis.

Proteins which were differentially expressed in the fibroblast of LHON cases, unaffected relatives and unrelated controls. Some sets of spots identified by MS/MS analysis in the same horizontal row were found to correspond to the same protein. Of the 61 differential-intensity spots, 33 spots representing 27 unique proteins were identified. Different isoforms of the protein mitofilin were represented by different spots in the gel. Seventeen proteins were differentially expressed between LHON cases and unrelated controls, and 24 proteins were differentially expressed between unaffected relatives of cases and unrelated controls (Table 2 and 3). Seven proteins were differently expressed between the LHON cases and their unaffected relatives (Table 4). An assessment of mitochondrial localization using the MitoMiner database [29] indicated that most of these identified proteins were mitochondrial resident proteins, and some had functional associations with mitochondria, though some were also localized in other compartments of the cell (Table 5).

Functions of the proteins were assessed using Nextprot [30]. The differentially expressed proteins could be classified in several groups: (1) those involved in intermediary metabolism (of carbohydrates, lipids and amino acids); (2) subunits of OXPHOS; (3) a cristae remodeling protein; (4) a protein involved in mitochondrial gene expression; (5) signal transduction; (6) chaperonins and proteases of the protein quality control system; (7) an antioxidant enzyme and (8) cytoskeletal structure (Table 5). All of these proteins were down-regulated in the mitochondrial fibroblast

Table 4. Summary of significantly altered proteins between the LHON cases and the unaffected relatives.

Spot ID	Protein name	Gene*	NCBI ID	Identification scores (MS/MS)	%Cov (MS/MS)	number of matched peptides (MS/MS)	emPAI	p/	MW (kDa)	Intensity (Mean ± SEM)		Fold change Affected/ unaffected	$P^{\#}$	FDR
										Affected (n = 7)	Unaffected (n = 3)			
295	major vault protein	MVP	gi|19913410	743	46	41	1.68	5.34	99.55	0.0519±0.0043	0.0273±0.0069	1.90	.033	0.018
300	lon protease homolog	LONP1	gi|21396489	1004	44	45	2.17	6.01	106.94	0.3006±0.0325	0.1572±0.0320	1.91	.031	0.018
587	Dihydrolipoamide Dehydrogenase And Dihydrolipoamide Dehydrogenase-Binding Protein (Didomain) Subcomplex Of Human Pyruvate Dehydrogenase Complex.	DLD	gi|83753870	563	51	28	2.86	7.95	54.18	0.1873±0.0124	0.1219±0.0050	1.54	.037	0.020
618	Glutamate Dehydrogenase-Apo Form	GLUD1	gi|20151189	743	65	40	5.02	7.66	56.32	0.3220±0.0353	0.1841±0.0300	1.75	.046	0.023
623	ATP synthase subunit alpha	ATP5A1	gi|4757810	1379	65	79	7.26	9.07	59.67	0.9932+0.0873	0.5828±0.1452	1.70	.025	0.015
693	ubiquinol-cytochrome c reductase core I protein	UQCRC1	gi|515634	382	52	22	2.38	5.94	52.59	0.2762±0.0135	0.1595±0.0194	1.73	.010	0.009
728	ubiquinol-cytochrome c reductase core I protein	UQCRC1	gi|515634	824	48	22	1.76	5.94	53.27	0.4247±0.0285	0.1948±0.0222	2.18	.001	0.003
862	Pyruvate dehydrogenase E1 component subunit alpha	PDHA1	gi|33357460	572	36	17	1.87	8.35	43.30	0.6067+0.0425	0.3537±0.0487	1.72	.004	0.006

*Gene name according to HUGO Gene Nomenclature Committee.

#indicates *P* value based on Post Hoc Tukey Test after one way ANOVA and the value less than 0.05 is considered significant in both tests.

doi:10.1371/journal.pone.0106779.t004

Table 5. Functional categories and sub-cellular localizations of proteins identified in the study based on the MitoMiner Database and Nextprot.

Proteins	Localization
Intermediary metabolism: TCA cycle and Carbohydrate Metabolism	
2-oxoglutarate dehydrogenase, mitochondrial isoform 1 precursor	M
Glycerol-3-phosphate dehydrogenase	M
Dihydrolipoyl dehydrogenase	M
Pyruvate dehydrogenase E1 component subunit alpha	M
Intermediary metabolism: Fatty acid Catabolism	
Methylmalonyl-CoA mutase	M
Trifunctional enzyme subunit alpha	M
Very long-chain specific acyl-CoA dehydrogenase	M
Propionyl-CoA carboxylase	M
Intermediary metabolism: Amino acid Metabolism	
Glutaminase	M
Glutamate dehydrogenase 1	M
Subunits of oxidative phosphorylation and electron transport function	
Succinate dehydrogenase [ubiquinone] flavoprotein subunit	M
Cytochrome b-c1 complex subunit 1	M
Electron transfer flavoprotein subunit alpha	M
ATP synthase subunit alpha	M
NADH dehydrogenase (ubiquinone) Fe-S protein 1, 75 kDa (NADH-coenzyme Q reductase)	M
Cristae remodeling	
Mitochondrial inner membrane protein	M
Mitochondrial Gene expression	
Leucine-rich PPR motif-containing protein	M
signal transduction	
Major vault protein	N, M
Glucosidase 2 subunit beta	ER
Protein stability and degradation of protein	
Lon protease homolog	M
Stress-70 protein, mitochondrial/Heat shock 70 kDa protein 9/MTHSP75	M, C
60 kDa heat shock protein, mitochondrial	M, C
Anti-oxidant enzymes	
Catalase	P, MI
cytoskeletal protein	
Vinculin	CSK
β-actin	CSK
Vimentin	CSK
Others	
Myosin-9/Cellular myosin heafvy chain-type A	C, M

M = Mitochondria, MI = Mitochondrial intermembrane space, ER = Endoplasmic Reticulum, C = Cytoplasm, N = Nucleus, CSK = cytoskeleton.
doi:10.1371/journal.pone.0106779.t005

proteomes of LHON patients and their unaffected relatives, compared with the unrelated controls.

However, expression levels of heat-shock protein 60, methylmalonyl-CoA mutase and myosin heavy chain were significantly different between the cases and the unrelated controls, but not between the unaffected relatives and the unrelated controls. Conversely, expression levels of 2-oxoglutarate dehydrogenase, NADH dehydrogenase (ubiquinone) Fe-S protein 1 (NDUFS1), ATP synthase subunit alpha, glutaminase, glutamate dehydrogenase, propionyl CoA carboxylase, beta-actin, glucosidase 2 subunit beta (PRKCSH) and vimentin were significantly different only between the unaffected relatives and the unrelated controls.

Expression of seven proteins differed significantly between the cases and their unaffected relatives: these were subunits of the respiratory chain such as ubiquinol cytochrome *c* reductase core I protein and ATP synthase subunits alpha; an enzyme of the TCA cycle, dihydrolipoamide dehydrogenase; one of the subunits of the pyruvate dehydrogenase complex; lon protease and major vault protein (Table 4).

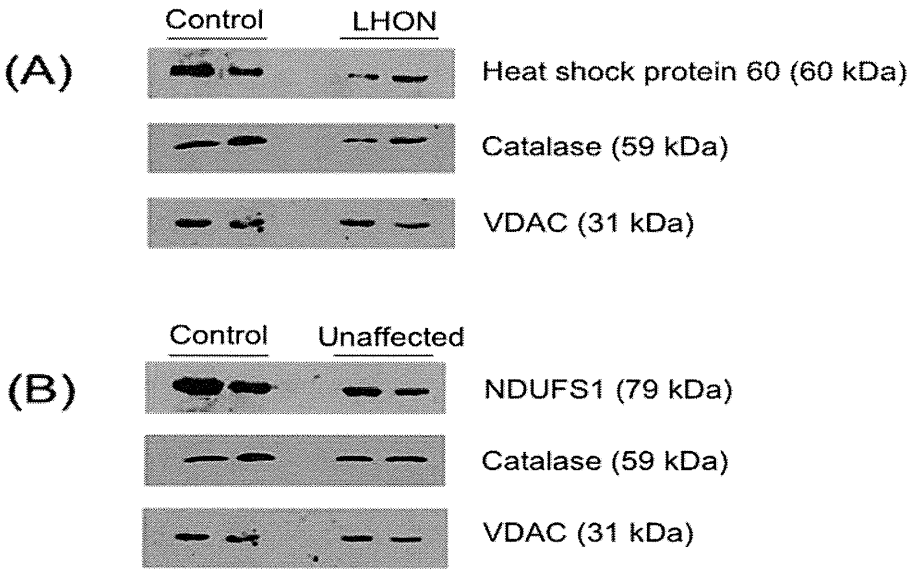

Figure 6. Validation of proteomic data by Western Blot analysis. These figures show: (A) The differentially expression of heat-shock protein 60 and catalase between LHON cases and controls; and (B) the differential expression of NDUFS1 and catalase between unaffected mutation carriers and controls. VDAC was used as a loading control. The two lanes represent samples from two different individuals for each group of samples.
doi:10.1371/journal.pone.0106779.g006

Validation of Proteomic data by Western Blot

To validate the differentially expressed proteins observed in the 2-DE proteomic analysis, three of the differentially expressed proteins - heat shock protein 60, catalase and NDUFS1 - were selected for western blot analysis. Compared with the unrelated controls, heat shock protein 60 and catalase were down-regulated in the mitochondrial fraction of the LHON cases, while catalase and NDUFS1 were down-regulated in the unaffected relatives. These differences all ran in the same direction as in the 2-DE proteomic analysis (Figure 6).

Discussion

It is impossible to sample retinal ganglion cells, the affected target cells of this mitochondrial disease. Hence in this study we used skin fibroblasts derived from the patients, which may mirror some of the features of other post-mitotic tissues such as retinal ganglial cells. The fibroblasts were cultured directly from the skin biopsies, from LHON patients and their unaffected relatives homoplasmic for the primary mtDNA mutation 11778G>A. The purity of the skin fibroblast cultures, which may contain epithelium, reticulocytes, and adipocytes, was confirmed using anti-Fibroblast surface protein. The skin fibroblasts were then used to explore the mitochondrial proteomes of these 11778G>A carriers, comparing them with the proteomes of control individuals using 2-DE with a non-linear IPG strip of pH 3–11.

The purity and the enrichment of the mitochondrial fraction were confirmed by western blotting with organelle-specific markers. The proteomics data also confirmed this, as most of the identified proteins were mitochondrial resident proteins. No mtDNA-encoded proteins, including PARL (hydrophobic and membrane bound protein) which was previously reported [27] were identified in this study, since these proteins are highly hydrophobic [31–33] and 2-DE does not provide good separation of hydrophobic and membrane bound proteins [34–36].

All of the proteins that were differentially expressed between 11778G>A carriers and unrelated controls were down-regulated in fibroblasts of 11778G>A carriers: either the LHON cases or their unaffected relatives (Figure 7). Some of the subunits of the OXPHOS complex were altered: NDUFS1 in complex I, succinate dehydrogenase in complex II, UQCRC1 in complex III and ATP5A1 in complex V were all down-regulated in fibroblasts of either the affected or the unaffected 11778G>A carriers. This was an unexpected finding since complex I defective LHON mutant cells may compensate for a lack of ATP synthesis through up-regulation of succinate/glycerol-3-phosphate dehydrogenase [37–39]. However, our results were in agreement with the findings of Qiang et al, where succinate/glycerol-3-phosphate driven respiration was reduced in mutant cells derived from some Chinese LHON families [40].

The proteins found to be significantly differently expressed between the cases, unaffected 11778G>A carriers and unrelated controls can be categorized functionally into 2 functional groups: bioenergetic pathways and mitochondrial protein quality control. A number of enzymes for intermediary metabolism were differentially expressed in 11778G>A mutant fibroblasts compared with unrelated controls (Table 2 and 3). Interestingly, differential expression was observed particularly in FAD-linked and NAD-linked dehydrogenases which produce reducing equivalents to feed the respiratory chain. For instance, altered expression was found for two enzymes of β-oxidation: FAD-dependent very long chain specific acyl-CoA dehydrogenase, and NAD-dependent trifunctional enzyme subunit alpha (also known as hydroxyacyl CoA dehydrogenase). And among the TCA cycle enzymes, FAD-dependent succinate dehydrogenase, NAD-dependent 2-oxoglutarate dehydrogenase, pyruvate dehydrogenase E1 component alpha subunit and dihydrolipoyl dehydrogenase were down-regulated in 11778G>A fibroblasts. Also down-regulated was glycerol-3-phosphate dehydrogenase, which is involved in transporting cytosolic reducing equivalents to the mitochondrial respiratory chain.